PERGAMON

Annals of Nuclear Energy 29 (2002) 1299–1313

annals of
NUCLEAR ENERGY

www.elsevier.com/locate/anucene

A non-stationary signal correlator for on-line transit time estimation

T. Tambouratzis*, M. Antonopoulos-Domis

Institute of Nuclear Technology, Radiation Protection, NCSR 'Demokritos', Aghia Paraskevi 153 10, Athens, Greece

Received 30 July 2001; accepted 24 August 2001

Abstract

The on-line reliable estimation and monitoring of transit time in BWRs is investigated. The interactive activation-competition artificial neural network is employed for providing an estimate of the current transit time directly at each incoming pair of signal values. As a result, transit time monitoring is accomplished for both constant and oscillating flow regimes, i.e. for both stationary and non-stationary signals. The proposed approach is robust to the presence of local and global component as well as to the addition of white uncorrelated noise.

1. Introduction

Transit time estimation and monitoring is of particular interest in boiling water reactors (BWRs), where the rising randomly fluctuating steam bubbles of the coolant constitute the principal excitation of the neutron density noise. For D_1 and D_2 a pair of axially separated neutron detectors placed in the same bypass channel and at a known distance from each other, the discretised neutron noise signals $s_1[i]$ and $s_2[i]$ ($i \in Z$ denotes the time index) can be represented as

$$\begin{aligned} s_1[i] &= l[i] + g[i] + n_1[i] \\ s_2[i] &= Al[i-\tau] + Bg[i] + n_2[i] \end{aligned} \tag{1}$$

* Corresponding author. Tel.: +30-1-65-03-748; fax: +30-1-65-33-431.
E-mail address: tatiana@ipta.demokritos.gr (T. Tambouratzis).

0306-4549/02/$ - see front matter
PII: S0306-4549(01)00112-8

where $l[i]$ denotes the local component that appears in $s_2[i]$ with a delay (transit time) τ with respect to its appearance in $s_1[i]$, $g[i]$ is the global component i.e. a coincident signal at both D_1 and D_2, $n_1[i]$ and $n_2[i]$ are uncorrelated random noise signals; A and B indicate that neither the local nor the global components are identical in the two signals.

The time required for the steam bubbles to travel from D_1 to D_2 is directly related to the coolant flow regime: the transit time is constant if the flow is constant, while it is periodic if periodic flow oscillation occurs. Concerning constant transit time, the traditionally employed technique is to correlate the stationary neutron noise signals $s_1[i]$ and $s_2[i]$ collected at D_1 and D_2, respectively: the maximum of the cross-correlation function (equivalently, the slope of the phase of the cross-spectrum) provides an estimate of the transit time. Unfortunately, the correlation technique: (a) requires a large number of consecutive signal values for reliable transit time estimation, (b) is sensitive to the local to global ratio (LGR) of the two components in $s_1[i]$ and $s_2[i]$, (c) cannot be applied to non-stationary signals, such as the neutron noise signals corresponding to time-varying transit times.

The application of artificial neural networks (ANNs, Tambouratzis et al., 1998) has been found capable of on-line transit time estimation and is robust to the presence of global component; furthermore, it can detect abrupt changes in the transit time. Recently, the evaluation of the average transit time in case of flow oscillations (where the correlation technique cannot be applied to the corresponding non-stationary neutron noise signals) has been investigated (Manera et al., 2000).

In this piece of research, the on-line reliable estimation and monitoring of transit time corresponding to stationary as well as non-stationary signals is tackled employing ANNs. A set of ANNs based on interactive activation and competition (IAC) has been employed and found capable of providing an estimate of the current transit time directly at each incoming pair of signal values (on-line operation); in this manner, transit time monitoring is accomplished for both constant and oscillating flow regimes. The proposed approach is robust to the presence of local and global component as well as to the addition of white uncorrelated noise.

2. Signal generation

The neutron noise signals (neutron density random fluctuations) have been simulated using a one-dimensional homogeneous, two neutron-group model. The model of Behringer et al. (1977) which accounts for both the local and the global components has been processed in the manner followed in Tambouratzis et al. (1998); here, constant as well as varying (periodically oscillating with constant amplitude, periodically oscillating with increasing amplitude, increasing whilst periodically oscillating with constant amplitude) velocity $V(t)$ of the steam bubbles has been implemented.

Assuming the reactor to be critical and using the static equations for the static fast and thermal neutron fluxes $\Phi_{10}(z)$ and $\Phi_{20}(z)$, respectively, the equations for the Fourier transforms $\delta\hat{\varphi}_1(z,\omega)$, $\delta\hat{\varphi}_2(z,\omega)$ of the fast flux fluctuation $\delta\varphi_1(z,t)$ and $\delta\varphi_2(z,t)$ of the thermal flux fluctuation read

$$\begin{bmatrix} D_1 \dfrac{\vartheta^2}{\vartheta z^2} - \Sigma_1(\omega) & \nu\Sigma_f u(\omega) \\ \Sigma_{12} & D_2 \dfrac{\vartheta^2}{\vartheta z^2} - \Sigma_2(\omega) \end{bmatrix} \cdot \begin{bmatrix} \delta\hat{\varphi}_1(z,\omega) \\ \delta\hat{\varphi}_2(z,\omega) \end{bmatrix} = \begin{bmatrix} \hat{S}_1 \\ \hat{S}_2 \end{bmatrix} \tag{2}$$

$$\Sigma_1(\omega) = \Sigma_{a1} + \Sigma_{12} + \frac{j\omega}{\upsilon_1};\ \Sigma_2(\omega) = \Sigma_{a2} + \frac{j\omega}{\upsilon_2};\ u(\omega) = 1 - \frac{j\omega\beta}{\lambda + j\omega} \tag{3}$$

where all symbols have their usual meaning, z is the vertical coordinate and $S_1(z,\omega)$, $S_2(z,\omega)$ are the sources of excitation induced by neutron cross-section fluctuations. Assuming that the main effect of moderator density fluctuations is through fluctuation $\delta\Sigma_{12}(z,t)$ of the removal cross-section Σ_{12}, that $\delta\Sigma_{12}(z,t)$ is proportional to the moderator fluctuation density, that the steam bubbles propagate upwards starting at the channel inlet and are not deformed between D_1 and D_2

$$\delta\hat{\Sigma}_{12}(z,\omega) = G.\delta\hat{a}_V(z,\omega) \tag{4}$$

where G is a proportionality constant and $\delta\hat{a}_V(z,\omega)$ is the Fourier transform of void fraction fluctuation at location z within the core (for $t = t_{\text{current}}$, the location z of the steam bubble which enters the core at t_o is given by $z = \int_{t_o}^{t_{\text{current}}} V(t).\mathrm{d}t$, where $V(t)$ is the velocity of all the steam bubbles in the core at time t). Then the excitations are

$$\begin{aligned} \hat{S}_1(z,\omega) &= G.\delta\hat{a}_V(z,\omega).\Phi_{10}(z) \\ \hat{S}_2(z,\omega) &= -G.\delta\hat{a}_V(z,\omega).\Phi_{10}(z) \end{aligned} \tag{5}$$

Let ψ_1, ψ_2 be the fast and thermal adjoint functions, respectively. Then $\delta\hat{\varphi}_2$ may be computed from

$$\begin{aligned} \delta\hat{\varphi}_2(z,\omega) &= \int_0^H [\psi_1(z,z',\omega).S_1(z',\omega) + \psi_2(z,z',\omega).S_2(z',\omega)]\mathrm{d}z' = \\ &= G.\int_0^H [\psi_1(z,z',\omega) - \psi_2(z,z',\omega)].\Phi_{10}(z').\delta\hat{a}_V(z',\omega).\mathrm{d}z' \end{aligned} \tag{6}$$

Now, for frequencies $\omega >> \lambda$ and $\omega << \upsilon_1(\Sigma_{a1} + \Sigma_{12})$, $\omega << \upsilon_2.\Sigma_{a2}$, which is very well satisfied for the frequencies of interest, Σ_1, Σ_2 and u of (3) may practically be taken to be real. Then, ψ_1 and ψ_2 are real and the inverse Fourier transform of (6) reads

$$\delta\varphi_2(z,t) = G.\int_0^H [\psi_1(z,z') - \psi_2(z,z')].\Phi_{10}(z').\delta a_V(z',t).\mathrm{d}z' \tag{7}$$

For the purposes of the simulation, integral (7) is evaluated numerically assuming that a new steam bubble b enters the bottom of the core at each time index $i \in Z$. All steam bubbles that are within the core at time i propagate upwards with the same

velocity $V[i]$.[1] By deriving the adjoint functions ψ_{1,D_1}, ψ_{1,D_2} and ψ_{2,D_1}, ψ_{2,D_2} from Behringer at al. (1977), the signals $s_1[i]$ and $s_2[i]$ corresponding to neutron detectors D_1 and D_2, respectively, at time i are given by

$$\begin{aligned} s_1[i] &= \sum_b \Phi_{10}(x[b,i]).\{\psi_{1,D_1}(x[b,i]) - \psi_{2,D_1}(x[b,i])\}.\delta\alpha_V[b,i] \\ s_2[i] &= \sum_b \Phi_{10}(x[b,i]).\{\psi_{1,D_2}(x[b,i]) - \psi_{2,D_2}(x[b,i])\}.\delta\alpha_V[b,i] \end{aligned} \tag{8}$$

where $x[b,i]$ is the position of steam bubble b at time i and $\delta a_V[b,i]$ is the implemented contribution of steam bubble b to the void fraction fluctuations at time i. The two signals are the model responses to the propagating disturbances δa_V and contain both the local and global components. An example is shown in Fig. 1 for a pair of neutron noise signals corresponding to the flow regime of periodically oscillating with increasing amplitude transit time.

3. ANNs for on-line transit time estimation

3.1. Proposed ANN approach

Assuming a given range of transit times $[\tau_{N1}, \tau_{N2}]$ with

$$\tau_j = h_j \Delta t, \quad j = N1, N1+1, ..., N2 \tag{9}$$

where Δt denotes the sampling interval ($h_j \in Z$ and $h_{j+1} = h_j + 1$, $j = N1, N1+1, ..., N2-1$), a set of overlapping ANNs has been implemented for transit time estimation. The employed ANNs stem from the IAC ANNs described in Grossberg (1987), Rumelhart and Zipser (1985), McClelland and Rumelhart (1988) and are constructed as follows [for more details the reader is referred to Tambouratzis et al. (1998)]:

- Each ANN [see Fig. 2(a)] comprises 10 nodes supporting a range of 10 consecutive transit times $[\tau_k, \tau_{k+9}]$; the jth node supports transit time τ_j ($j = k, k+1, ..., k+9$). Every node is characterized by a positive connection to itself (self-excitation) and by negative connections to all other nodes (lateral inhibition). The emergent ANN connectivity enforces interaction through competition and the winner-take-all regime.
- Each ANN node receives as inputs the two measured signals s_1 and s_2 and assumes continuous activation values corresponding to these inputs; for the jth

[1] Although $V[i]$ is not necessarily constant over i, it is the same for all steam bubbles at a given i. Therefore, the distance between consecutive steam bubbles remains constant over time. The distance between pairs of neighbouring steam bubbles is the same for all pairs when $V[i]$ is constant; it varies between pairs when $V[i]$ is not constant.

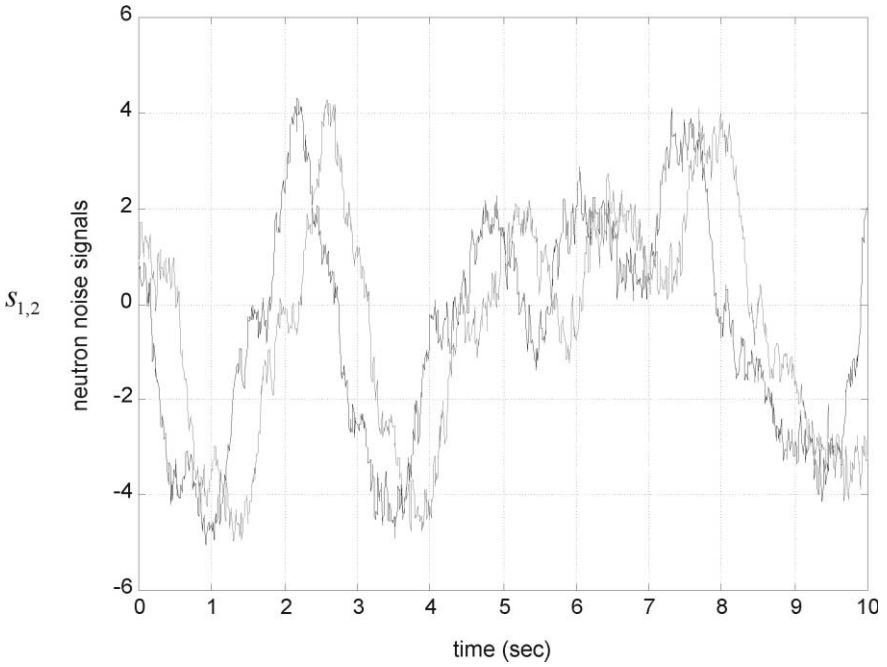

Fig. 1. Neutron noise signals s_1 and s_2 collected at D_1 (dark line) and D_2 (light line), respectively, for the flow regime of oscillating with increasing amplitude transit time.

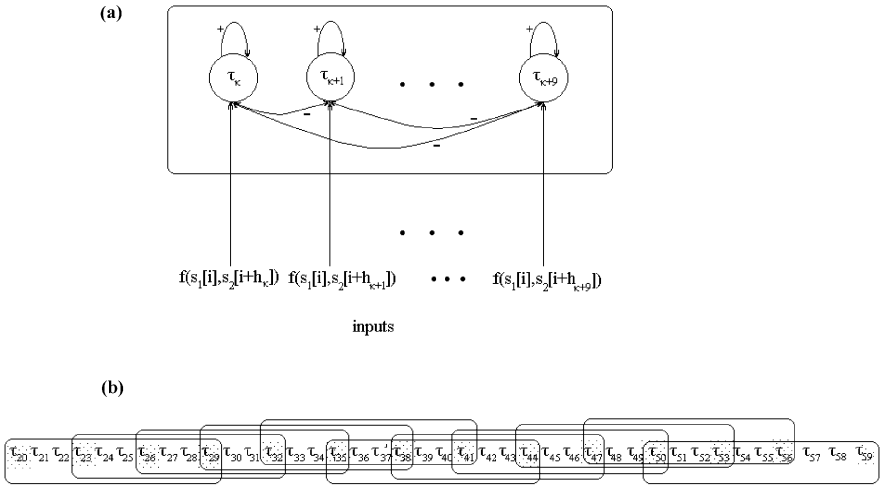

Fig. 2. ANN supporting $[\tau_k, \tau_{k+9}]$ (a); set of 11 overlapping ANNs supporting $[\tau_{21}, \tau_{58}]$ (b).

node, the ith input constitutes a function $f(s_1[i], s_2[i + h_j])$ of the similarity between neutron noise signals $s_1[i]$ and $s_2[i + h_j]$. Owing to lateral inhibition, nodes with high activation values tend to suppress nodes with low activation

values; suppression results in stability concerning both the existence/identity of the winner and the activation values of the ANN nodes. In order to modulate stability, the activation values of the nodes decay at each input: in case of a change in the inputs, the decay allows the appropriate (previously non-winner) node to become the winner.

- Exactly three kinds of ANN decisions are allowed:
  - Absolute decision. A winner is found whose activation value is the highest among all nodes and exceeds a set threshold ϑ; the activation values of all other nodes are significantly below ϑ. The transit time supported by the winner constitutes the ANN absolute decision.
  - Tentative decision. A winner is found whose activation value is the highest among all nodes and exceeds ϑ; the activation values of the other nodes do not exceed ϑ, but at least one node exists whose activation value is very close to ϑ. The transit time supported by the winner constitutes the ANN tentative decision.
  - No-decision. No winner is found; either no or more than one activation value exceeds ϑ.
- The IAC ANN parameters (e.g. decay, ϑ) are chosen so as to:
  - reduce erroneous absolute decisions at the expense of a greater number of tentative decisions and no-decisions,
  - accomplish robustness (stability of the winner to insignificant fluctuations in transit time, e.g. small amounts of noise) and sensitivity (quick changes of the winner to variations in transit time).

The set of ANNs has been constructed so as to fully cover the given range of transit times $[\tau_{N1}, \tau_{N2}]$, with neigbouring ANNs overlapping by seven transit times; there is no restriction on the number of ANNs in the set. The following are performed for the final estimation of the transit time:

- *Filtering*. The decisions of the outer two nodes (one on each side, supporting transit times τ_k and τ_{k+9}) of each ANN are discarded. This is performed in order to avoid erroneous decisions in cases where the actual transit time is just outside the range supported by the ANN and the corresponding outer node becomes the winner.
- *Combination*. The estimated transit time at Δt is given by a majority vote of the absolute and tentative decisions of the set of ANNs in the window [Δt-4, Δt-3, Δt-2, Δt-1, Δt], i.e. the window extending $4\Delta t$ before the current Δt. Hence, an estimation of the transit time is made at each Δt by considering the recent history of the ANN decisions (from which the current final estimation cannot significantly deviate). It is mentioned that, owing to the implemented overlap between ANNs,[2] discarding the decisions of an outer node of a given ANN

[2] For full coverage, the lowest transit time of the first ANN is selected between τ_{N1-1}, τ_{N1-2} or $\tau_{N1\text{-}3}$ while the highest transit time of the last ANN is selected between τ_{N2+1}, τ_{N2+2} or τ_{N2+3}.

does not affect the final estimation: the transit time supported by the outer node is also estimated by the two neighbouring ANNs in the direction of the outer node.

3.2. Tests-results

Pairs of neutron noise signals corresponding to four flow regimes (for constant, oscillating with constant amplitude, oscillating with increasing amplitude, decreasing whilst oscillating with constant amplitude transit time) have been employed. For the tests presented here, $\Delta t = 0.01$ s, the actual transit time varies in the range [21 Δt, 58 Δt] and the period of oscillation equals 3 s (i.e. is of the same order of magnitude as the transit time). Eleven ANNs have been constructed in the manner described in Section 3.1 [Fig. 2(b)], covering the range [20 Δt, 59Δt]. After filtering, the transit times equalling 21 Δt, 22 Δt, 23 Δt, 56 Δt, 57 Δt and 58 Δt fall within the range of exactly one ANN, while the remaining transit times fall within the range of either two or three ANNs.

For transit times varying in the manner of the representative examples (thin, dark lines) of Fig. 3(a–d), the following have been observed concerning the filtered decisions of each ANN.

(1) When the transit time falls within the range of the ANN, accurate and fast detection of (constant) transit time as well as transit time monitoring (i.e. following its variations) are accomplished. The proportion of absolute, tentative and no-decisions is 10.65, 61.55 and 27.9%, respectively; 100% of the absolute decisions and 85.39% of the tentative decisions correctly detect the actual transit time. Tentative decisions, no-decisions as well as erroneous estimations of the transit time occur more often near variations of the transit time than when the transit time is kept constant; no more than 2 Δt are required until an (absolute or tentative) decision is made at the beginning of ANN operation or in case of a variation in the actual transit time.

(2) Consistent no-decision when the transit time falls outside the range of the ANN. The proportion of absolute, tentative and no-decisions is 0.52, 13.51 and 85.97%, respectively; the absolute and tentative decisions correspond to random winners at random Δt. The sparseness and randomness of the winners, together with the high proportion of no-decisions, constitute indicators that the actual transit time falls outside the range of the ANN.

Concerning the final estimation, Fig. 3 depicts the estimated transit time (thick, light lines) overlapped with the actual transit time (thin, dark lines) for one representative test from each flow regime; in all regimes, significant deviations (>3 Δt) are observed for isolated Δt only.[3] The ability to estimate the current transit time as well as to quickly follow its variations—no matter how small—is of special interest for BWR stability monitoring. The accuracy of the proposed approach is further shown in Table 1, averaged over all tests and separately for the four flow regimes; the decline in accuracy during changes of the transit time (especially rapid ones)

[3] These deviations can be safely discarded due to the assumption of gradual change in transit time between consecutive Δt.

becomes obvious by comparing the averaged results for the constant flow regime with those of the other three flow regimes.

Increasing the global component causes graceful degradation of each ANN (fall in the speed and accuracy of the decisions, decline in the proportion of absolute decisions, increase in the proportion of tentative decisions and no-decisions) as well as of

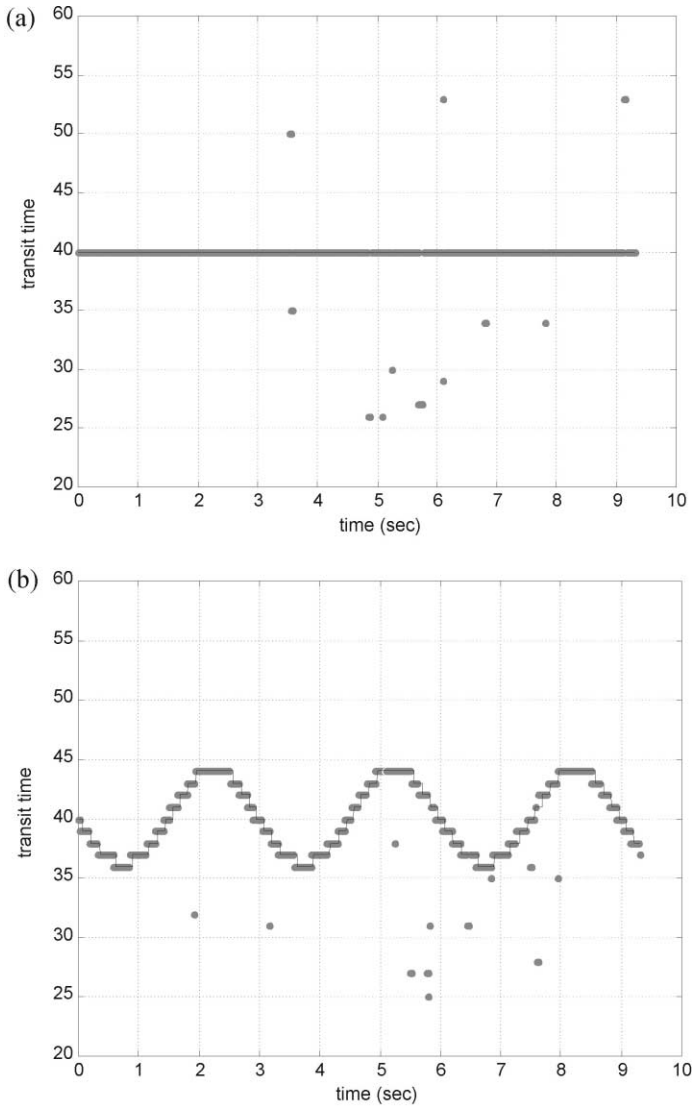

Fig. 3. Representative examples of transit time estimation for the flow regimes of constant (a), oscillating with constant amplitude (b), oscillating with increasing amplitude (c), and decreasing whilst oscillating with constant amplitude (d) transit time; estimated transit time (thick, light lines) overlapped with the actual transit time (thin, dark lines).

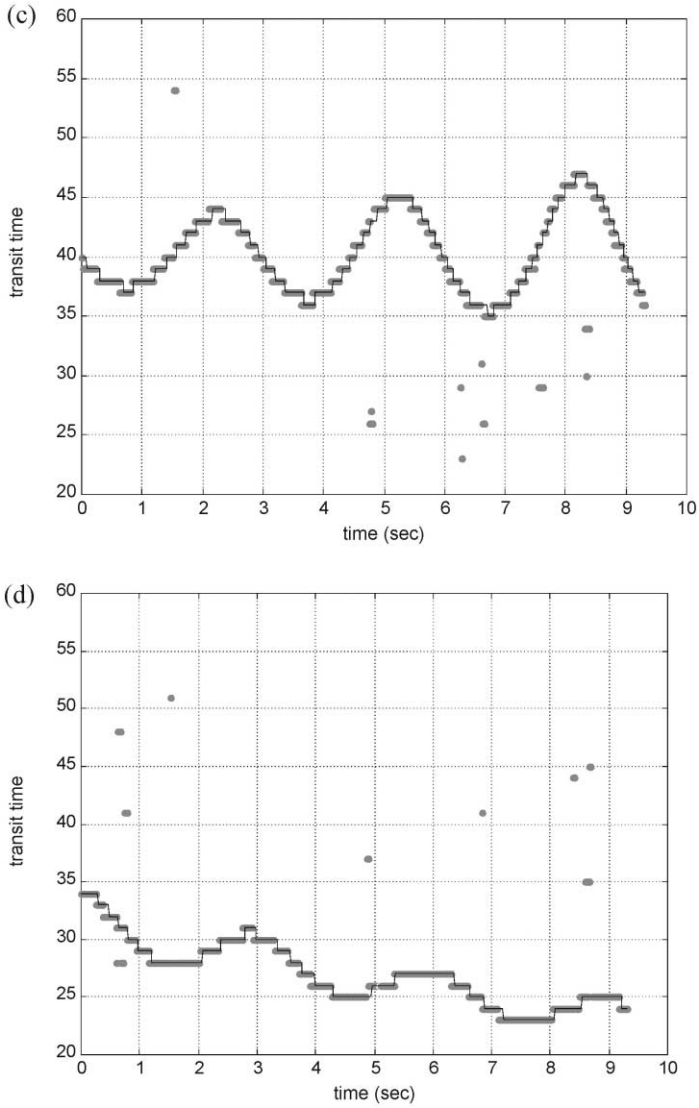

Fig. 3. (*continued*).

Table 1
Average proportion of deviations between actual and estimated transit time for the four flow regimes

Deviation (%) flow regime	0 Δt	$\pm 1\ \Delta t$	$\pm 2\ \Delta t$	$\pm 3\ \Delta t$	$>3\ \Delta t$
Constant	96.67	1.03	0.77	0.44	1.09
Oscillating (const. amplit.)	73.98	23.44	0.67	0.71	1.2
Oscillating (incr. amplit.)	67.8	29.03	1.07	0.92	1.18
Decreasing and oscillating (const. amplit.)	84.41	12.04	1.19	1.28	1.08

the final estimation (decrease in accuracy). The results concerning the flow regime of oscillating with increasing amplitude transit time are presented here (the results for the constant flow regime are superior, while those for the other two non-constant flow regimes are comparable). Fig. 4 depicts the estimated transit time (thick, light lines) overlapped with the actual transit time (thin, dark lines) for selected LGR

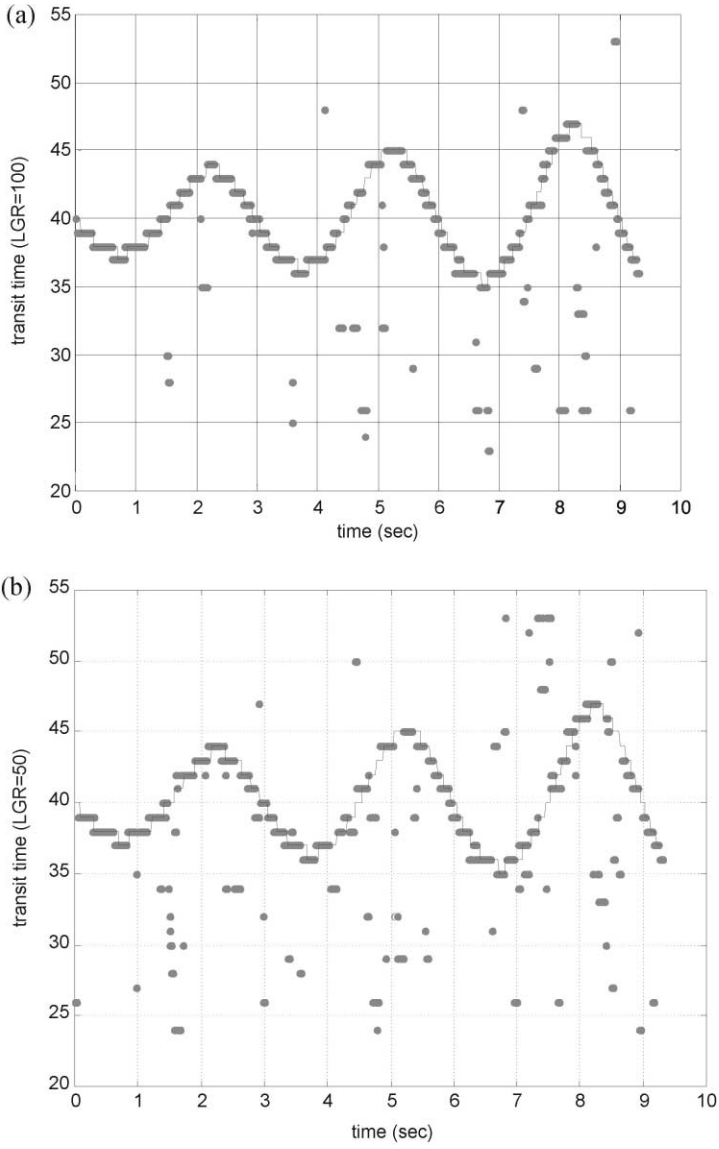

Fig. 4. An example of the effect of increasing amounts of global component on transit time estimation for the flow regime of oscillating with increasing amplitude transit time; estimated transit time (thick, light lines) overlapped with the actual transit time (thin, dark lines) for LGR = 100, 50, 25 and 15.

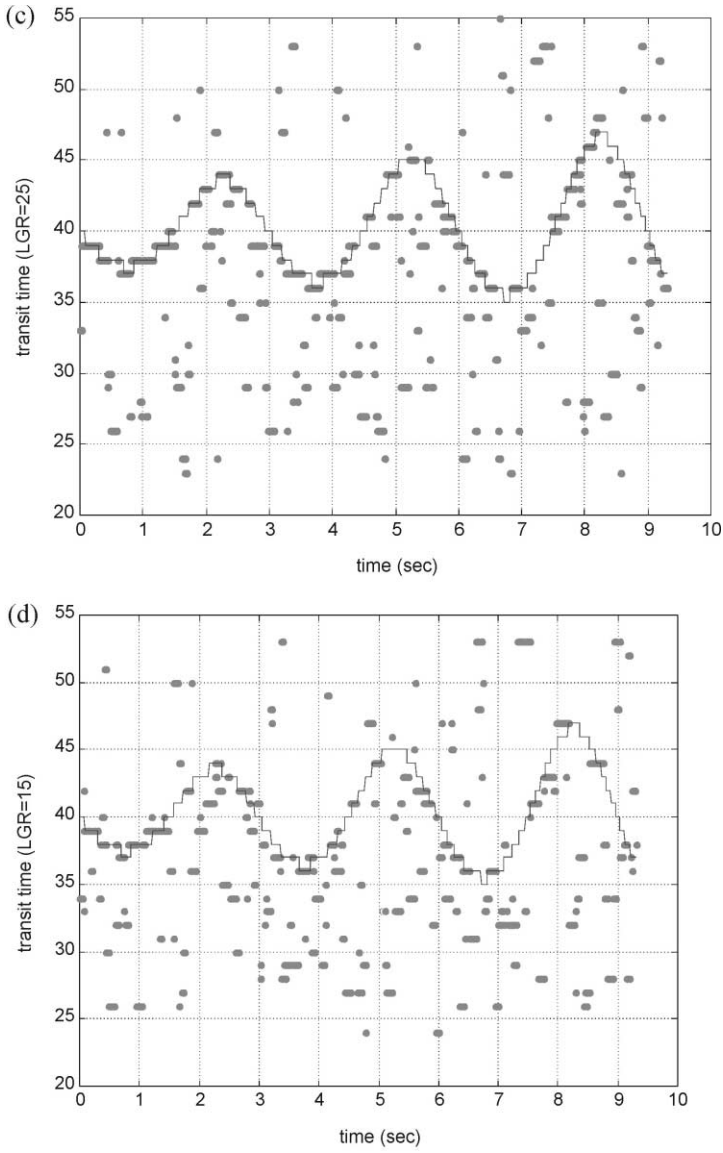

Fig. 4. (*continued*)

levels of added global component and demonstrates the gradual deterioration of the final estimation. As the LGR of the added global component decreases, significant deviations between actual and estimated transit time occur more frequently and for longer time intervals; while for LGR levels greater than 20 the actual transit time can be detected and monitored, for LGR levels lower than that transit time

estimation deteriorates significantly, as expected. The fall in accuracy of the final estimation is further demonstrated in Table 2 for decreasing LGR levels.

The results corresponding to the presence of increasing amounts of local component are not described here as they are (for all flow regimes) slightly better than those detailed above for the global component. The results concerning the addition

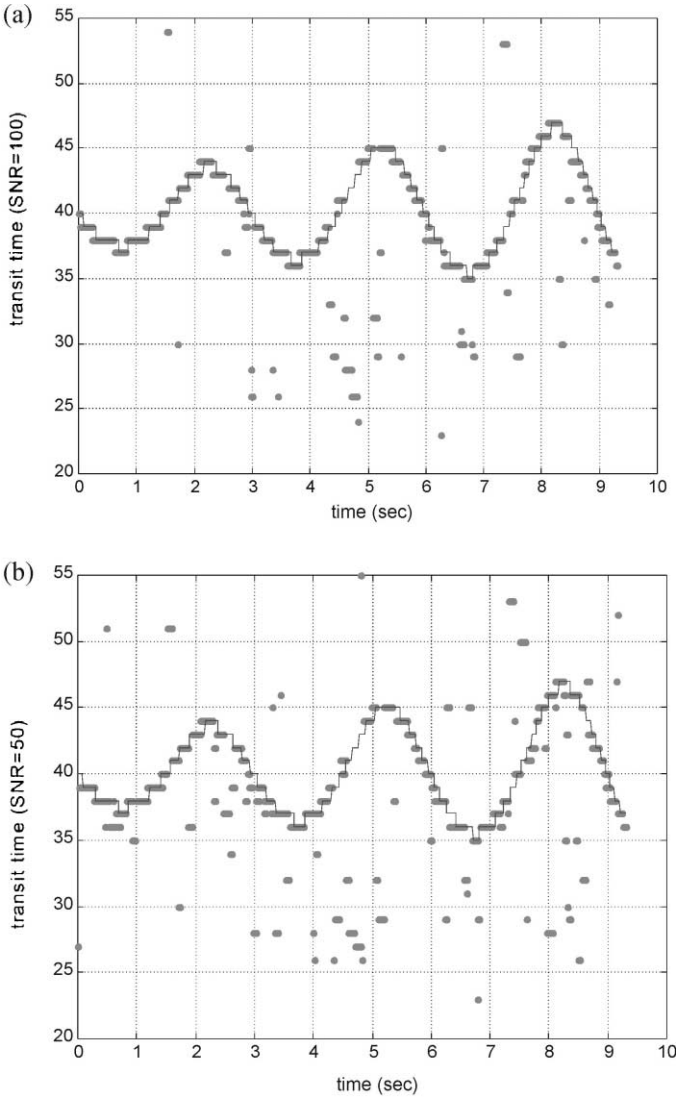

Fig. 5. An example of the effect of increasing amounts of uncorrelated white noise on transit time estimation for the flow regime of oscillating with increasing amplitude transit time; estimated transit time (thick, light lines) overlapped with the actual transit time (thin, dark lines) for SNR = 100, 50, 25 and 15.

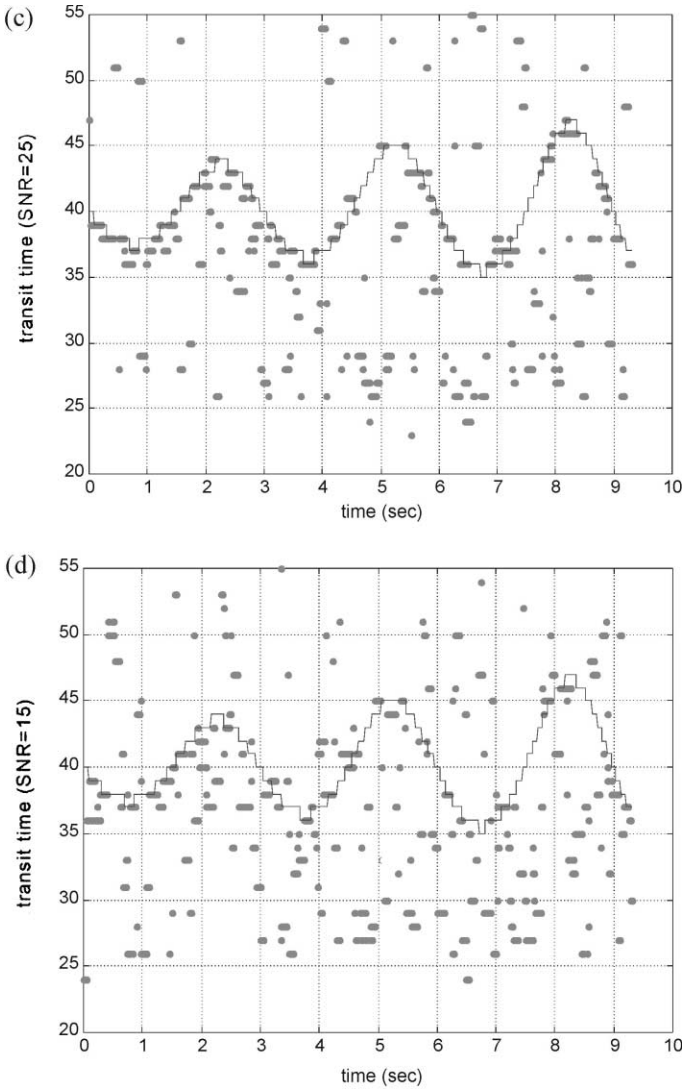

Fig. 5. (*continued*)

of white uncorrelated noise to the two signals are shown in Fig. 5 and Table 3 for SNR levels corresponding to the LGR levels of the global component. Although comparable numerically (at least for levels up to 25) to the results concerning the presence of global component, the results are viewed as slightly worse. This is owing to the more even distribution of the estimations, whereby the assumption of gradual change in transit time between consecutive Δt cannot always be employed for detecting (and discarding) the erroneous estimations.

Table 2
Average proportion of deviations between actual and estimated transit time for varying LGR levels of added global component; flow regime of oscillating with increasing amplitude transit time

Deviation (%) LGR	0 Δt	± 1 Δt	± 2 Δt	± 3 Δt	>3 Δt
∞	67.8	29.03	1.07	0.92	1.18
100	57.42	30.43	0.32	0.11	11.72
50	47.85	29.57	1.56	2.8	18.22
25	30.86	18.82	4.41	6.02	39.89
15	20.65	6.77	4.95	6.01	61.62

Table 3
Average proportion of deviations between actual and estimated transit time for varying SNR levels of uncorrelated white noise; flow regime of oscillating with increasing amplitude transit time

Deviation (%) SNR	0 Δt	± 1 Δt	± 2 Δt	± 3 Δt	>3 Δt
∞	67.8	29.03	1.07	0.92	1.18
100	56.77	28.71	1.9	1.34	11.28
50	49.25	25.59	2.26	2.26	20.64
25	24.73	22.58	8.06	13.77	30.86
15	14.73	17.53	7.58	14.46	45.7

4. Conclusions

The use of a set of overlapping IAC ANNs for constant as well as periodic transit time estimation and monitoring has been investigated. Owing to its competitive nature, the proposed approach has been found capable of providing an on-line reliable estimate of the current transit time directly at each incoming pair of signal values; in this manner, transit time monitoring is accomplished for both constant and oscillating flow regimes, i.e. for both stationary and non-stationary signals. The proposed approach is robust to the presence of local and global component as well as to the addition of white uncorrelated noise.

References

Behringer, K., Kosaly, G., Kostic, L., 1977. Theoretical investigation of the local and global components of the neutron noise field in a BWR. Nucl. Sci. Eng. 63, 306.

Grossberg, S., 1987. Competitive learning: from interactive activation to adaptive resonance. Cogn. Sci. 11, 23.

Manera, A., van der Hagen T.H.J.J, de Kruijf, W.J.M., van Dam, H., On the determination of transit times during flow oscillations, Proceedings of the International Meeting on reactor Noise, 11–13 October 2000, Athens, Greece, p. 301.

McClelland, J.L., Rumelhart, D.E., 1988. Explorations in parallel distributed processing: a Handbook of Models, Programs, and Exercises. MIT Press, Cambridge, MA.

Rumelhart, D.E., Zipser, D., 1985. Feature discovery by competitive learning. Cogn. Sci. 9, 75.

Tambouratzis, T., Antonopoulos-Domis, M., Marseguerra, M., Padovani, E., 1998. On-line estimation of transit time using artificial neural networks. Nucl. Sci. Eng 130, 113.